Propagation of Fundamental Mode in Regularly Bending Multi-Mode Waveguides

Hongyan Yu
Westlake University
Xinyu Sun
Westlake University
Dasai Ban
Westlake University
Feng Qiu (qiufeng@westlake.edu.cn)
Westlake University

Research Article

Keywords: Multi-mode waveguides, bending waveguides, photonic integrated circuits

Posted Date: February 9th, 2021

DOI: https://doi.org/10.21203/rs.3.rs-179989/v1

Version of Record: A version of this preprint was published at Optical and Quantum Electronics on July 14th, 2021. See the published version at https://doi.org/10.1007/s11082-021-03069-6.

Propagation of Fundamental Mode in Regularly Bending Multi-mode Waveguides

Hongyan Yu[1,2,3], Xinyu Sun[1,2,3], Dasai Ban[2,3], and Feng Qiu[2,3]

[1] Zhejiang University, Hangzhou 310027, Zhejiang Province, China
[2] Key Laboratory of 3D Micro/Nano Fabrication and Characterization of Zhejiang Province, School of Engineering, Westlake University, 18 Shilongshan Road, Hangzhou 310024, Zhejiang Province, China
[3] Institute of Advanced Technology, Westlake Institute for Advanced Study, 18 Shilongshan Road, Hangzhou 310024, Zhejiang Province, China

E-mail: qiufeng@westlake.edu.cn

Abstract

Transmission of the fundamental mode in multi-mode waveguides is an effective scheme for a silicon-based platform to reduce scattering loss. However, the application of the scheme is usually limited to straight waveguides and restricted in multi-mode bending waveguides. This is because the fundamental mode of a straight waveguide is seriously disordered after passing the bend. In this work, we have presented a "matched bending radius" approach, by which an ultra-low loss and negligible modal disorder have been demonstrated in the Si and Si_3N_4 multi-mode waveguides. The estimated optical field overlap factor is almost 0 dB at the matched bending radius, indicating that the fundamental mode can be re-generated after passing the multi-mode bending waveguide. The proposed approach will contribute to applying the low loss scheme in large-scale photonic integrated circuits.

Keywords: Multi-mode waveguides, bending waveguides, photonic integrated circuits

1 Introduction

Photonic integrated circuits (PICs) have been remarkably successful in supporting the explosive growth of information technology over the past decades(Luo et al. 2014). For promoting developments in high-density PICs, silicon (Si) and silicon nitride (Si_3N_4) waveguides are attracting much attention, due to their relatively high refractive index and fabrication process compatible with the complementary metal-oxide semiconductor. On the other hand, the high refractive index also result in greater propagation loss mainly dominated by the waveguide sidewall scattering(Lee et al. 2000). For example, typical propagation loss ranges from 0.5 to 3.0 dB/cm for single-mode Si waveguides and 0.2 to 2.0 dB/cm for Si_3N_4 waveguides(Lee et al. 2001; Xia et al. 2007). This may limit the performance of devices longer than a few centimeters. According to the Payne-Lacey model(Payne,Lacey 1994), the scattering loss is proportional to the portion of the mode overlapping with the waveguide sidewalls. In order to minimize the modal interaction with the sidewalls, it has been shown that low propagation loss can be achieved by propagating the fundamental mode in a large size multi-mode waveguide(Frigg et al. 2019). By using this scheme, propagation loss as low as 0.085 and 0.0013 dB/cm has been presented in the Si and Si_3N_4 multi-mode waveguides, respectively(Guillén-Torres et al. 2014; Ji et al. 2017).

To achieve a flexible and compact layout, bending waveguides, especially 90° bends, are inevitable in PICs. Though the fundamental mode can propagate stably in a multi-mode straight waveguide(Wang et al. 2018), the modal field usually becomes distorted significantly after passing a multi-mode bending waveguide(Musa et al. 2004; Li et al. 2019; Berlatzky et al. 2005; Subramaniam et al. 1997). This is caused by the modal mismatch between the straight and bending sections, which excites high-order modes in the bending waveguide. Serious model distortion may restrict the applications of the above low loss scheme in PICs. To overcome the model distortion, some methods have been suggested, mainly including using a deliberately designed Euler bending(Vogelbacher et al. 2019), curving a straight multi-mode waveguide 90° bend based on transformation optics and etching a sub-wavelength grating in the bent section [15-17](Gabrielli et al. 2012; Xu,Shi 2018; Wu et al. 2019). It is still an issue, however, to propagate the fundamental mode in a normally bending multi-mode waveguide without any specially design.

In this work, we present a straightforward "matched bending radius" approach, which enables the fundamental mode to be propagated in a regularly bending multi-mode waveguide with a small radius. The presented approach can be applied to both Si and Si_3N_4 multi-mode waveguides with a broad wavelength range of 100 nm. The potential application in large-scale PICs has also been discussed via demonstrating cascaded 90° bending waveguides. The obtained results should be attractive to the flexible application of the above low loss scheme.

2 Matched bending radius in multi-mode bending waveguides

To demonstrate the "matched bending radius" approach, Si and Si_3N_4 multi-mode waveguides with typical dimensions have been considered [11, 18-20](Li et al. 2019; Luke et al. 2013; Qiu et al. 2015; Seok et al. 2019), as shown in Table-I. All the simulated waveguides consist of an input/output straight waveguide and a regular 90° arc-bend, as shown in Fig. 1. 3D finite-difference time-domain method was used to simulate the light propagation and the mode field distribution.

Table-I Parameters of Si and Si_3N_4 waveguide

Waveguide	Width (W) (μm)	Thickness (T) (μm)	Supporting modes	Group
Si	2.0	0.22	4	A
		0.05	2	B
Si_3N_4	2.5	0.4	2	C
		0.9	3	D

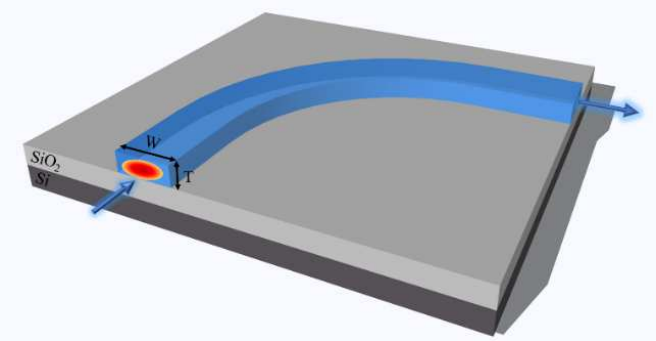

Fig. 1. Schematic of a regularly 90° bending multi-mode waveguide: the dimensions are given in Table-I

In the simulations, the launched light is set as TE_0 mode to excite only the fundamental mode in the input waveguide. Figure 2(a) exhibits the simulated light propagation in the Si waveguides of Group-A with different radii. With a random bending radius of 9 μm, high-order modes are excited in the bending section and a superposition of these modes happens at the output. Therefore, we can see that the output field becomes seriously distorted. One intuitive method is to enlarge the bending radius. However, the result is still unfavorable with a distorted output field when the radius is increased to 23 μm.

In contrast, with a smaller radius of 14.5 μm, we find that the light can be propagated with a negligible distortion after passing the 90° regular arc-bend. This radius is named as "matched bending radius". In order to investigate the "matched bending radius" more clearly, the output model profiles with various radii are shown in Fig. 2(b). For comparison, the model distribution of the input TE_0 mode is also given. The output optical field at the "matched bending radius" overlap with the input TE_0 mode very well, but deviates obviously for the random radius =9 or 23 μm.

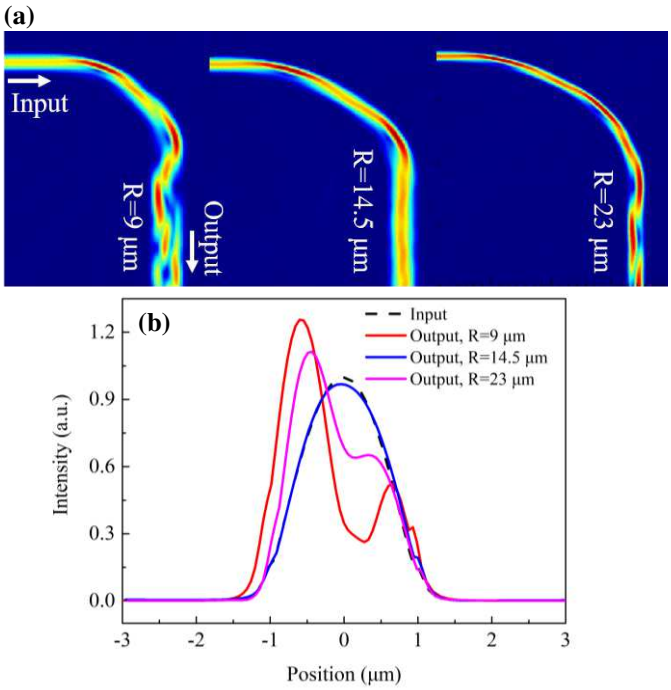

Fig. 2. (a) Simulated light propagation in Group-A waveguides (matched bending radius R=14.5 μm). (b) Modal field distribution in the output waveguides with different radii R.

To evaluate the availability of the "matched bending radius" approach in different waveguides, we define an optical field overlap factor Γ as:

$$\Gamma = 10 \times log_{10} \frac{P_{TE0-out}}{P_{TE0-in}} \quad (1)$$

where $P_{TE0\text{-}out}$ and $P_{TE0\text{-}in}$ are the TE_0 mode power of the output and the input field, respectively. Since the input field has been set as TE_0 mode, Γ should be 0 dB when neither optical loss nor model distortion is induced after the light passing the multi-mode bending waveguide.

Figures 3(a) and (b) show the obtained Γ of the Si and Si_3N_4 waveguides listed in Table-I at the wavelength λ of 1.55 μm. One unique feature is that $\Gamma \approx 0$ dB is achieved successfully at the matched bending radius for all the waveguides, which proves the availability of the "matched bending radius" approach. Another feature is that the matched radius arises periodically, which may be explained as follows. When the TE_0 mode of the input straight waveguide enters the bend, higher modes are excited in the bending multi-mode waveguide. These higher modes propagate independently with different phase velocities. Afterward, these modes combine in the output multi-mode waveguide. At the matched bending radius, the phase velocity difference among these modes is close to $2n\pi$, so the output field almost overlaps with the input TE_0 mode. In the case of high refractive index Si waveguides, the first matched radius of Si waveguides is near 14 μm. For the Si_3N_4 waveguides, a larger matched bending radius is achieved around 19 μm.

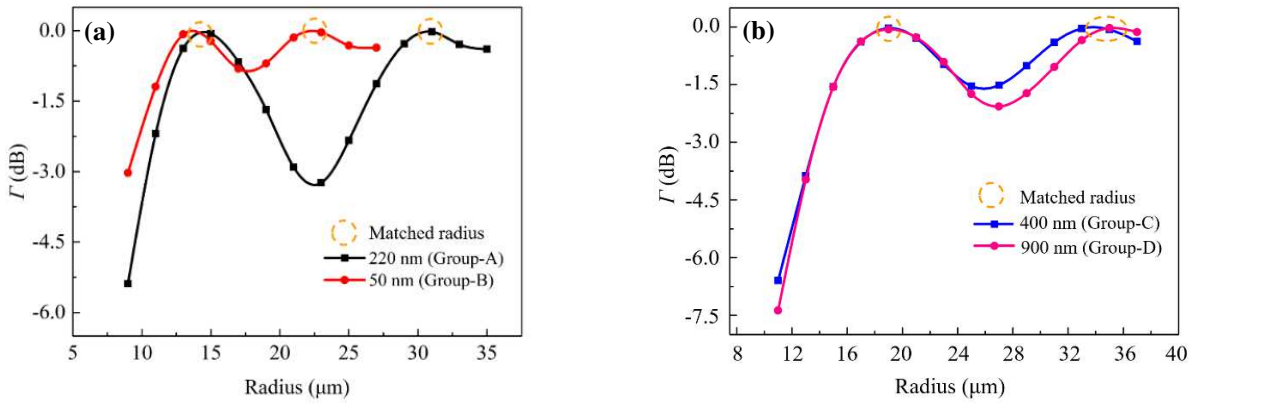

Fig. 3. Calculated optical field overlap factor Γ of (a) Si and (b) Si_3N_4 bending waveguides (λ=1.55 μm).

An important factor for the application of the "matched bending radius" approach is wavelength dependent performance. The transmission spectra of the TE_0 mode propagating at the matched radius are shown in Fig. 4(a) and (b). For comparison, the spectra at random radii of 23 and 17 μm for Group A-B and 27 μm for Group C-D are also plotted. From the spectra, we can see that Γ is close to 0 dB for all the waveguides at the "matched bending radius" in the broadband from 1.5 to 1.6 μm. This means that the ultra-low optical loss and inter-mode crosstalk can be achieved by using the "matched bending radius" approach. In contrast, the mode distortion keeps serious for any random radii over a wide range of 100 nm. This wavelength range covers the whole C and L-band of the fiber-optic communication, which may be useful for future telecommunication development.

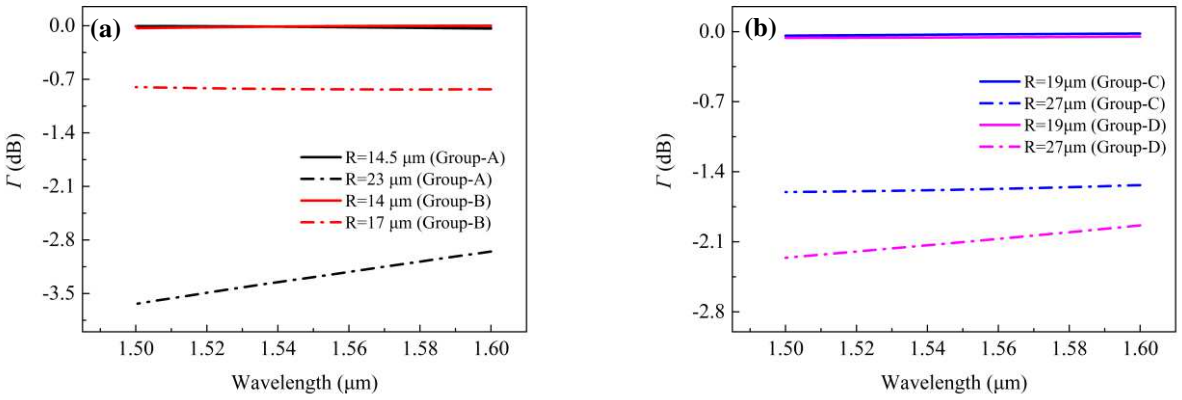

Fig. 4. Wavelength dependent Γ variation at the matched radius and random radius (a) Si waveguides and (b) Si_3N_4 waveguides (Solid line: matched radius, dash line: random radius).

In PICs, there may be several bending waveguides to connect numerous optical devices. Consequently, we check the propagation of TE_0 mode in 20 cascaded 90° multi-mode bending waveguides as shown in Fig. 5(a). Figure 5 (b) and (c) show the results of Group-C at the bending radius of 19 μm (matched radius) and 27 μm (random radius), respectively. It is obvious that the TE_0 mode is almost re-generated after passing the cascaded 90° bending multi-mode waveguides with a matched bending radius, but seriously distorted with a random radius. Similar performances were also found for waveguides in Groups A, B, and D.

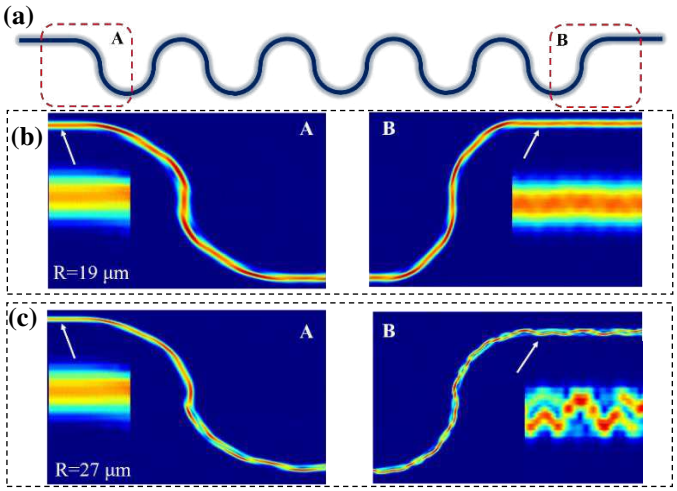

Fig. 5. Simulated light propagation of TE_0 mode along 20 cascaded 90° bends: (a) Schematic, (b) at the matched radius R=19 μm and (c) at a random radius R=27 μm.

3 Conclusion

We have presented a "matched bending radius" approach enabling the fundamental mode to be propagated in a regular 90°bending multi-mode waveguide. For the Si and Si_3N_4 multi-mode waveguides with typical dimensions, after passing a 90° bend, the output mode almost overlaps with the input TE_0 mode at the "matched bending radius" over a wavelength range of 100 nm. The "matched bending radius" is not only suitable for a single bend but also for multiple 90° bends. The presented approach provides a simple solution to reduce the significant model distortion in multi-mode bending waveguides, which should be attractive to widely apply the low loss scheme of propagating the fundamental mode in a large size multi-mode waveguide.

Acknowledgements

This work was supported by National Natural Science Foundation of China (62075184).

References

Berlatzky, Y., Shtrichman, I., Narevich, R., Narevicius, E., Rosenblum, G., Vorobeichik, I.: Controlling coupling of guided to radiating modes using adiabatic transitions between waveguides of different curvature. J. Lightwave Technol. **23**(3), 1278-1283 (2005). doi:10.1109/JLT.2004.840006

Frigg, A., Boes, A., Ren, G., Abdo, I., Choi, D.-Y., Gees, S., Mitchell, A.: Low loss CMOS-compatible silicon nitride photonics utilizing reactive sputtered thin films. Opt. Express **27**(26), 37795-37805 (2019). doi:10.1364/OE.380758

Gabrielli, L.H., Liu, D., Johnson, S.G., Lipson, M.: On-chip transformation optics for multimode waveguide bends. Nature Communications **3**, 1217 (2012). doi:10.1038/ncomms2232

Guillén-Torres, M.A., Caverley, M., Cretu, E., Jaeger, N.A.F., Chrostowski, L.: Large-area, high-Q SOI ring resonators. In: 2014 IEEE Photonics Conference, 12-16 Oct. 2014 2014, pp. 336-337

Ji, X., Barbosa, F.A.S., Roberts, S.P., Dutt, A., Cardenas, J., Okawachi, Y., Bryant, A., Gaeta, A.L., Lipson, M.: Ultra-low-loss on-chip resonators with sub-milliwatt parametric oscillation threshold. Optica **4**(6), 619-624 (2017). doi:10.1364/OPTICA.4.000619

Lee, K.K., Lim, D.R., Kimerling, L.C., Shin, J., Cerrina, F.: Fabrication of ultralow-loss Si/SiO2 waveguides by roughness reduction. Opt. Lett. **26**(23), 1888-1890 (2001). doi:10.1364/OL.26.001888

Lee, K.K., Lim, D.R., Luan, H.-C., Agarwal, A., Foresi, J., Kimerling, L.C.: Effect of size and roughness on light transmission in a Si/SiO2 waveguide: Experiments and model. Applied Physics Letters **77**(11), 1617-1619 (2000). doi:10.1063/1.1308532

Li, C., Liu, D., Dai, D.: Multimode silicon photonics. Nanophotonics **8**(2), 227-247 (2019). doi:10.1515/nanoph-2018-0161

Luke, K., Dutt, A., Poitras, C.B., Lipson, M.: Overcoming Si3N4 film stress limitations for High Quality factor ring resonators. Opt. Express **21**(19), 22829-22833 (2013)

Luo, L.-W., Ophir, N., Chen, C.P., Gabrielli, L.H., Poitras, C.B., Bergmen, K., Lipson, M.: WDM-compatible mode-division multiplexing on a silicon chip. Nature Communications **5**(1), 3069 (2014). doi:10.1038/ncomms4069

Musa, S., Borreman, A., Kok, A.A.M., Diemeer, M.B.J., Driessen, A.: Experimental study of bent multimode optical waveguides. Appl. Opt. **43**(30), 5705-5707 (2004). doi:10.1364/AO.43.005705

Payne, F.P., Lacey, J.P.R.: A theoretical analysis of scattering loss from planar optical waveguides. Optical and Quantum Electronics **26**(10), 977-986 (1994)

Qiu, F., Sato, H., Spring, A.M., Maeda, D., Ozawa, M.-a., Odoi, K., Aoki, I., Otomo, A., Yokoyama, S.: Ultra-thin silicon/electro-optic polymer hybrid waveguide modulators. Applied Physics Letters **107**(12), 123302 (2015). doi:10.1063/1.4931490

Seok, T.J., Kwon, K., Henriksson, J., Luo, J., Wu, M.C.: Wafer-scale silicon photonic switches beyond die size limit. Optica **6**(4), 490-494 (2019). doi:10.1364/OPTICA.6.000490

Subramaniam, V., Brabander, G.N.D., Naghski, D.H., Boyd, J.T.: Measurement of mode field profiles and bending and transition losses in curved optical channel waveguides. J. Lightwave Technol. **15**(6), 990-997 (1997). doi:10.1109/50.588672

Vogelbacher, F., Nevlacsil, S., Sagmeister, M., Kraft, J., Unterrainer, K., Hainberger, R.: Analysis of silicon nitride partial Euler waveguide bends. Opt. Express **27**(22), 31394-31406 (2019). doi:10.1364/OE.27.031394

Wang, L., Xie, W., Van Thourhout, D., Zhang, Y., Yu, H., Wang, S.: Nonlinear silicon nitride waveguides based on a PECVD deposition platform. Opt. Express **26**(8), 9645-9654 (2018). doi:10.1364/OE.26.009645

Wu, H., Li, C., Song, L., Tsang, H.-K., Bowers, J.E., Dai, D.: Ultra-Sharp Multimode Waveguide Bends with Subwavelength Gratings. Laser & Photonics Reviews **13**(2), 1800119 (2019). doi:10.1002/lpor.201800119

Xia, F., Sekaric, L., Vlasov, Y.: Ultracompact optical buffers on a silicon chip. Nature Photonics **1**(1), 65-71 (2007). doi:10.1038/nphoton.2006.42

Xu, H., Shi, Y.: Ultra-Sharp Multi-Mode Waveguide Bending Assisted with Metamaterial-Based Mode Converters. Laser & Photonics Reviews **12**(3), 1700240 (2018). doi:10.1002/lpor.201700240

Figures

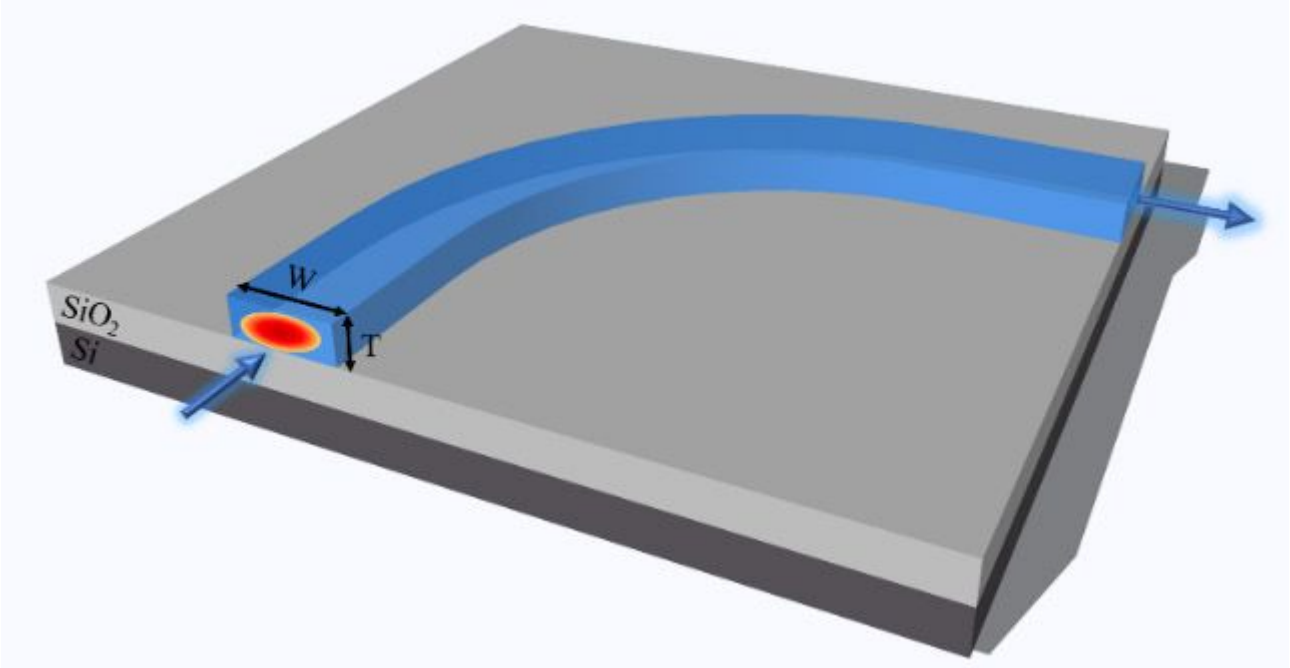

Figure 1

Schematic of a regularly 90° bending multi-mode waveguide: the dimensions are given in Table-

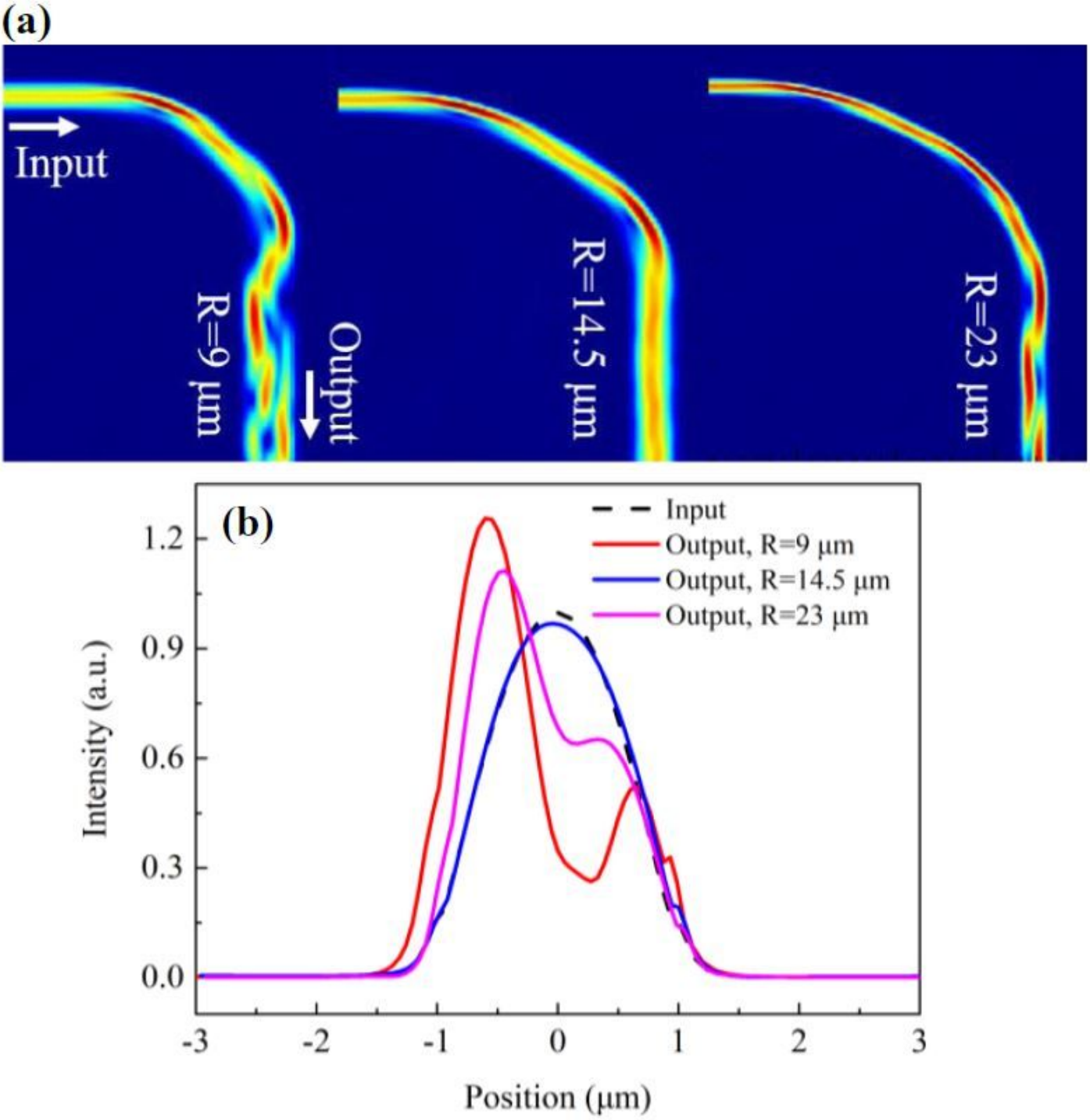

Figure 2

(a) Simulated light propagation in Group-A waveguides (matched bending radius R=14.5 μm). (b) Modal field distribution in the output waveguides with different radii R.

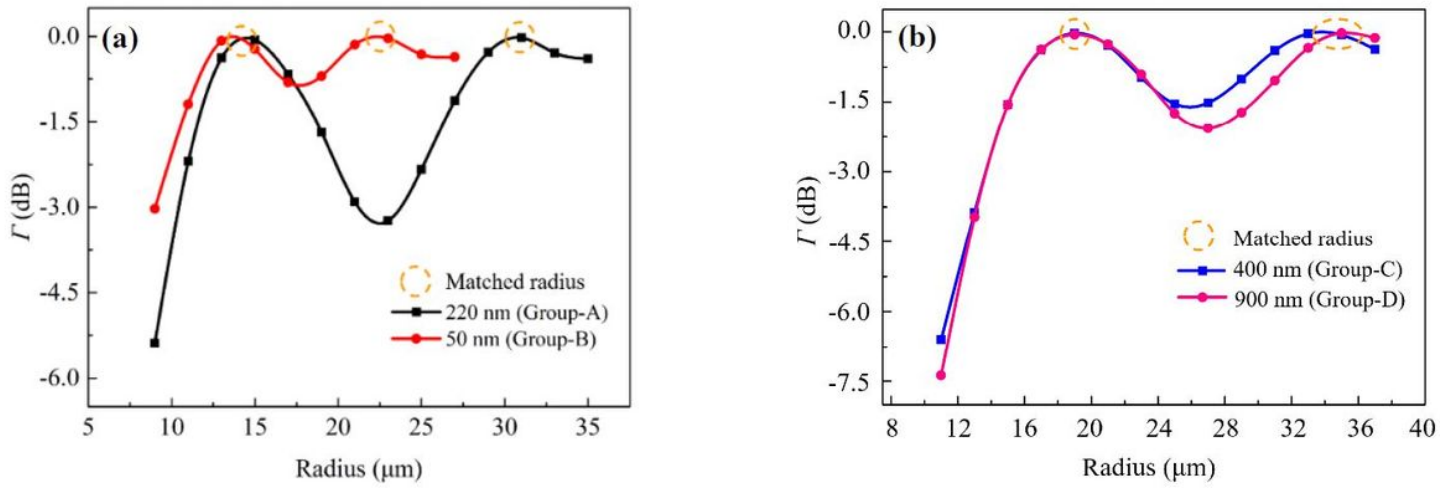

Figure 3

Calculated optical field overlap factor Γ of (a) Si and (b) Si3N4 bending waveguides (λ=1.55 μm).

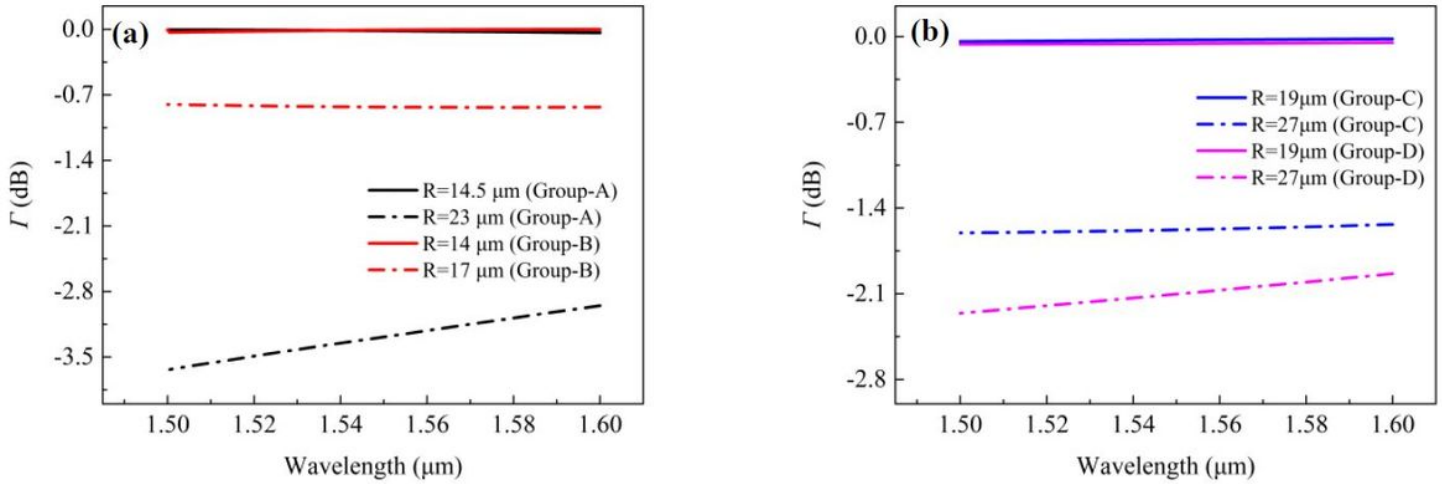

Figure 4

Wavelength dependent Γ variation at the matched radius and random radius (a) Si waveguides and (b) Si3N4 waveguides (Solid line: matched radius, dash line: random radius).

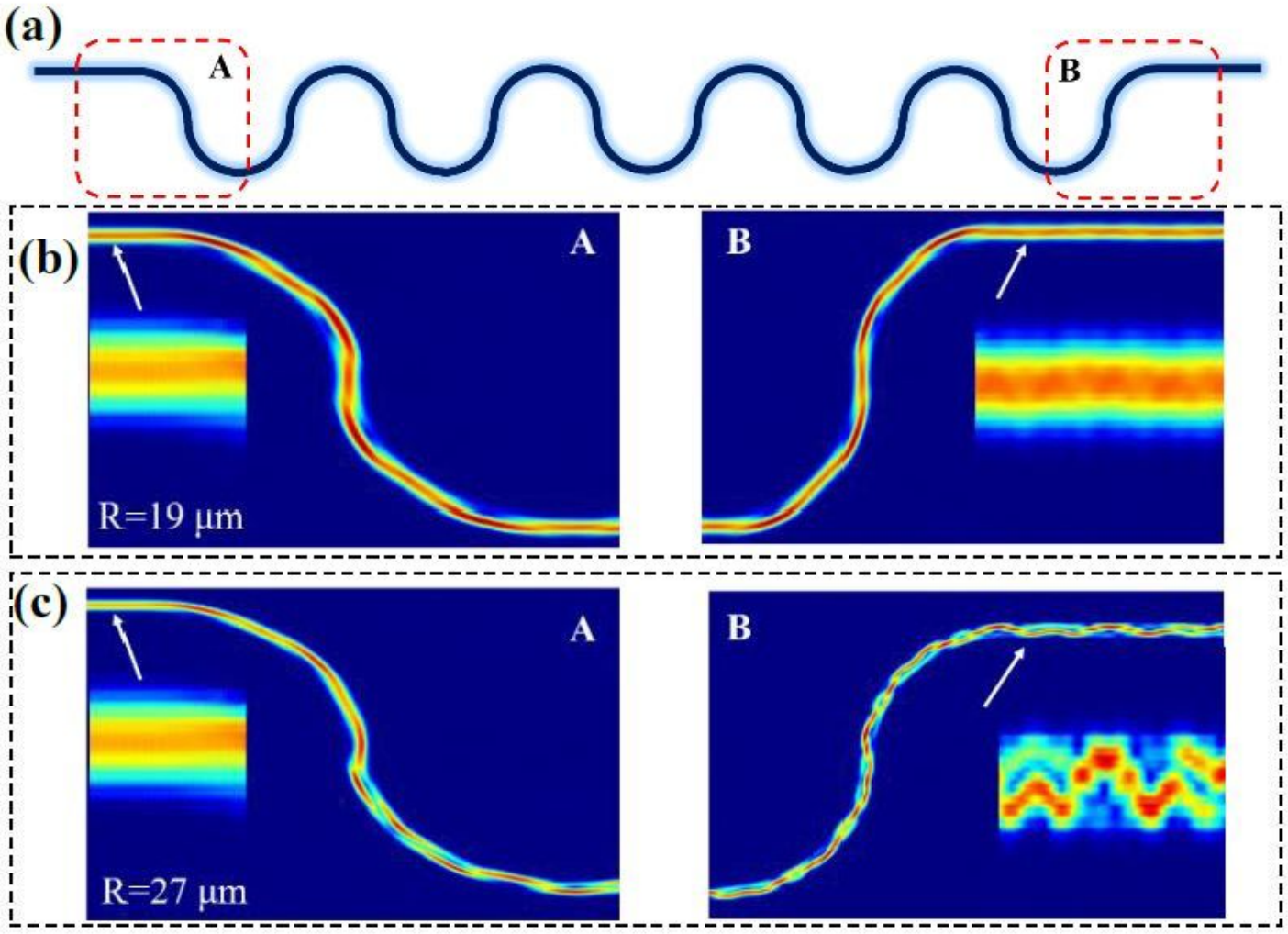

Figure 5

Simulated light propagation of TE0 mode along 20 cascaded 90° bends: (a) Schematic, (b) at the matched radius R=19 μm and (c) at a random radius R=27 μm.